Virologica Sinica 39 (2024) 459–468

Contents lists available at ScienceDirect

Virologica Sinica

journal homepage: www.keaipublishing.com/en/journals/virologica-sinica
www.virosin.org

Research Article

Development of a Měnglà virus minigenome and comparison of its polymerase complexes with those of other filoviruses

Shi-Zhe Xie [a,b], Ke Yao [a,b], Bei Li [a], Cheng Peng [a], Xing-Lou Yang [c,d,*], Zheng-Li Shi [a,*]

[a] State Laboratory of Virology, Wuhan Institute of Virology, Chinese Academy of Sciences, Wuhan, 430071, China
[b] University of Chinese Academy of Sciences, Beijing, 100049, China
[c] Yunnan Key Laboratory of Biodiversity Information, Kunming Institute of Zoology, Chinese Academy of Sciences, Kunming, 650201, China
[d] Hubei Jiangxia Laboratory, Wuhan, 430200, China

ARTICLE INFO

Keywords:
Bat filovirus
Měnglà virus (MLAV)
Minigenome
Replication
Antiviral drug screening

ABSTRACT

Ebola virus (EBOV) and Marburg virus (MARV), members of the *Filoviridae* family, are highly pathogenic and can cause hemorrhagic fevers, significantly impacting human society. Bats are considered reservoirs of these viruses because related filoviruses have been discovered in bats. However, due to the requirement for maximum containment laboratories when studying infectious viruses, the characterization of bat filoviruses often relies on pseudoviruses and minigenome systems. In this study, we used RACE technology to sequence the 3′-leader and 5′-trailer of Měnglà virus (MLAV) and constructed a minigenome. Similar to MARV, the transcription activities of the MLAV minigenome are independent of VP30. We further assessed the effects of polymorphisms at the 5′ end on MLAV minigenome activity and identified certain mutations that decrease minigenome reporter efficiency, probably due to alterations in the RNA secondary structure. The reporter activity upon recombination of the 3′-leaders and 5′-trailers of MLAV, MARV, and EBOV with those of the homologous or heterologous minigenomes was compared and it was found that the polymerase complex and leader and trailer sequences exhibit intrinsic specificities. Additionally, we investigated whether the polymerase complex proteins from EBOV and MARV support MLAV minigenome RNA synthesis and found that the homologous system is more efficient than the heterologous system. Remdesivir efficiently inhibited MLAV as well as EBOV replication. In summary, this study provides new information on bat filoviruses and the minigenome will be a useful tool for high-throughput antiviral drug screening.

1. Introduction

Taxonomically, filoviruses belong to the order *Mononegavirales*, a large group of enveloped viruses whose genomes are made up of a negative-strand, non-segmented RNA molecule. The International Committee on Taxonomy of Viruses divided the *Filoviridae* family into eight genera: *Cuevavirus*, *Dianlovirus*, *Orthoebolavirus*, *Orthomarburgvirus*, *Oblavirus*, *Striavirus*, *Tapjovirus*, and *Thamnovirus*, with the former four found in bats and humans and the latter in fish (Negredo et al., 2011; Shi et al., 2018; Kuhn et al., 2019; Yang et al., 2019; Horie, 2021; Kemenesi et al., 2022). While the Reston virus (RESTV) causes recessive infection in humans, other members of *Orthoebolavirus* and *Orthomarburgvirus*, previously named *Ebolavirus* and *Marburgvirus*, can cause severe hemorrhagic fevers in humans and animals (Rougeron et al., 2015; Kuhn et al., 2019). Because of the high morbidity and mortality rates and lack of efficient vaccines and therapeutics, human filoviruses are classified as biosafety level 4 pathogens. Bats are considered natural reservoirs of *Cuevavirus*, *Dianlovirus*, *Orthoebolavirus*, and *Orthomarburgvirus* (Olival and Hayman, 2014; Yang et al., 2019; Koch et al., 2020). Despite of the wealth of information we have obtained about bat filovirus, our understanding of MLAV is still insufficient.

Měnglà virus (MLAV), the only member of the newly established genus *Dianlovirus*, was discovered in *Rousettus amplexicaudatus* in Měnglà County, Yunnan Province, China. We previously sequenced the nearly complete genome of MLAV, excluding the 3′-leader and 5′-trailer sequences (Yang et al., 2019). The coding region of MLAV is 18,330 nucleotides long and shares 32%–54% nucleotide identity with known bat and human filoviruses. The MLAV genome structure is consistent with that of other filoviruses, encoding seven proteins in the following order from the 3′-end to the 5′-end of the genome: nucleoprotein (NP),

* Corresponding authors.
E-mail addresses: zlshi@wh.iov.cn (Z.-L. Shi), yangxinglou@mail.kiz.ac.cn (X.-L. Yang).

https://doi.org/10.1016/j.virs.2024.03.011
Received 6 December 2023; Accepted 25 March 2024
Available online 21 May 2024

polymerase cofactor (VP35), matrix protein (VP40), glycoprotein (GP), transcription factor (VP30), nucleocapsid maturation protein (VP24), and RNA-dependent RNA polymerase (L). NP is a nucleocapsid protein that binds to viral nucleic acids and plays an important role in genome replication. VP40 and VP24 are structural proteins that form the internal virion structure. L protein is a replication enzyme that combines with VP30, VP35, and NP to form a replication complex, providing key functions for virus replication, transcription, and translation (Muhlberger, 2007; Martin et al., 2017; Cao et al., 2023). Using the vesicular stomatitis virus-based pseudovirus assay, we demonstrated that MLAV uses the same receptor, Niemann-Pick C1, as Ebola virus (EBOV) and Marburg virus (MARV) for cell entry. In addition, we found that MLAV pseudovirus can enter cell lines derived from different animals and humans (Yang et al., 2019). These findings have suggested that MLAV has the potential for interspecies infection in humans and other animals.

Minigenomes are useful tools for studying the genome transcription and replication of RNA viruses without the need for live virus manipulation, particularly for those viruses that cannot be cultured *in vitro* or require high-level biosafety containment (Hoenen et al., 2011). Studies have shown that the viral non-coding region is essential for viral replication, the terminal sequences of the 3′-leaders of filoviruses are species-specific (Manhart et al., 2018; Deflube et al., 2019) and the conformation of the EBOV trailer and its interaction with host factors affect the viral lifecycle (Sztuba-Solinska et al., 2016). In this study, we refined the previously constructed MLAV minigenome using newly obtained 3′-leader and 5′-trailer sequences and analyzed the effects of homogenous and heterogeneous 3′-leader and 5′-trailer sequences from other filoviruses, as well as the inhibitor remdesivir, on replication activity. We expected our study to provide a useful tool for studying MLAV genome transcription and replication, as well as for antiviral drug screening.

2. Materials and methods

2.1. Cells

HEK293 (ATCC #CRL-1573) cells were maintained in Dulbecco's modified Eagle's medium (Gibco, Waltham, MA, USA) supplemented with 10% fetal bovine serum (Gibco) at 37 °C in the presence of 5% CO_2.

Immortalized renal cells of *R. leschenaultia* (RlKi), *Pteropus alecto* (PaKi) (Luo et al., 2021) and *R. amplexicaudatus* (RoaKi) were maintained in Dulbecco's modified Eagle medium/Nutrient Mixture F-12 (Gibco, Waltham, MA, USA) supplemented with 10% fetal bovine serum (Gibco) at 37 °C in the presence of 5% CO_2. *R. amplexicaudatus* (RoaKi) was immortalized according to previously reported methods (Crameri et al., 2009).

2.2. Plasmids

All cDNA clones used in this study were generated by PCR using Q5 high-fidelity DNA polymerase (NEB, Ipswich, MA, USA). EBOV and MARV minigenome systems were constructed as reported previously (Watt et al., 2014; Yang et al., 2019). To complete the MLAV genome, the MLAV 3′-leader and 5′-trailer sequences were measured using HiScript-TS 5′/3′ RACE kit (Vazyme, Nanjing, China) and M-MLV Reverse Transcriptase (Promega, Madison, USA). To construct the MLAV minigenome with enhanced green fluorescent protein (EGFP) reporter gene, the MLAV trailer-L 3′ UTR-EGFP-NP 5′ UTR-leader sequence was synthesized and cloned into the pGEM vector using a ClonExpress II One Step Cloning Kit (Vazyme, Nanjing, China), and the support plasmids (NP, VP30, VP35, L) were cloned into the pCAGGS vector. The EGFP gene was replaced with a NanoLuc reporter for antiviral drug screening.

To construct chimeric MLAV minigenome systems, the 5′-trailer and 3′-leader of the MLAV minigenome were replaced with those of EBOV and MARV, respectively, using the ClonExpress II One Step Cloning Kit. The support plasmids of RNPs are not codon-optimized for EBOV, MARV, and MLAV systems. The chimeric minigenomes were annotated 3E5E, 3E5D, 3D5E, 3D5M, 3M5D and 3M5M (E: EBOV, D: MLAV, M: MARV).

2.3. Virus sequences

The following NCBI reference filovirus sequences were used for sequence comparison: Měnglà dianlovirus isolate Rousettus-wt/CHN/2015/Sharen-Bat9447-1, complete genome (GenBank: KX371887.2); Zaire ebolavirus isolate Ebola virus/H. sapiens-tc/COD/1976/Yambuku-Mayinga, complete genome (NC_002549.1); Tai Forest ebolavirus isolate Tai Forest virus/H. sapiens-tc/CIV/1994/Pauleoula-CI, complete genome (NC_014372.1); Bundibugyo ebolavirus, complete genome (NC_014373.1), Sudan ebolavirus strain Boniface, complete genome (FJ968794.1); Reston ebolavirus isolate Reston virus/M. fascicularis-tc/USA/1989/Philippines89-Pennsylvania, complete genome (NC_004161.1); Marburg marburgvirus isolate Marburg virus/H. sapiens-tc/KEN/1980/Mt. Elgon-Musoke, complete genome (NC_001608.3); and Bombali ebolavirus isolate Bombali ebolavirus/Mops condylurus/SLE/2016/PREDICT_SLAB000156, complete genome (NC_039345.1).

2.4. Optimization of minigenome system

HEK293 cells were seeded in a 24-well plate at 4×10^5 cells/well. To optimize the concentration of support plasmids in MLAV minigenome replication system, the cells were co-transfected with different amount of NP or L plasmid, along with VP35 (62.5 ng), VP30 (37.5 ng), minigenome plasmid (500 ng), and pCAGGS-T7/Pol plasmid expressing the T7 RNA polymerase (125 ng), using FuGene6 (Promega, Madison, WI, USA). After determining the optimal ratio of NP and L plasmid, the ratio of other components in the minigenome replication system was further adjusted to achieve the highest level of minigenome reporter gene activity.

To determine whether VP30 is necessary for MLAV minigenome replication system, cells were co-transfected with support plasmids (260 ng L, 350 ng NP, 100 ng VP35), T7 polymerase plasmid (125 ng), MLAV minigenome plasmid (500 ng), with or without VP30 (30 ng). The replication system omitted the L plasmid was set as the negative control. The NanoLuc luciferase activity was measured at 48 h post-transfection.

In order to investigate the efficiency of MLAV minigenomes with different terminal bases and the expression efficiency of minigenome systems in different cells, we co-transfected minigenome plasmid with EGFP reporter (500 ng), support plasmids (260 ng L, 350 ng NP, 100 ng VP35, and 30 ng VP30), and T7 polymerase plasmid (125 ng) into HEK293, RlKi, PaKi or RoaKi cells. To quantify the transfection efficiency of minigenome system containing different terminal bases in different cells, we co-transfected minigenome plasmids with NanoLuc reporter (500 ng), support plasmids (260 ng L, 350 ng NP, 100 ng VP35, and 30 ng VP30), T7 polymerase plasmid (125 ng), and a plasmid containing firefly luciferase (pNL4-3-luc-R-E) (500 ng, as the internal control for transfection efficiency) into cells. The activity of NanoLuc luciferase in the minigenome system and the activity of firefly luciferase were measured at 48 h post-transfection. The fold change was calculated using the following equation: Nanoluc fluorescence value in experimental group/fluorescence value of firefly luciferase.

In order to investigate whether the minigenome system of MLAV, MARV, and EBOV are compatible with each other, we co-transfected minigenome plasmid (500 ng) of MLAV, MARV, and EBOV with homologous or heterologous support plasmids and T7 polymerase plasmid (125 ng), and then observed EGFP expression at 48 h after transfection. For the EBOV minigenome system, the following amounts of support plasmid were added to each transfection mix: 500 ng L, 62.5 ng NP, 62.5 ng VP35, and 37.5 ng VP30. For the MARV minigenome system, 500 ng L, 500 ng NP, 50 ng VP35, and 50 ng VP30 plasmids were added to each transfection mix. For the MLAV minigenome system, 260 ng L, 350 ng NP, 100 ng VP35, and 30 ng VP30 plasmids were added to each transfection mix. For the comparison of chimeric minigenome efficiency, we

co-transfected 500 ng chimeric minigenome and MLAV support plasmids with 125 ng T7 polymerase plasmid into HEK293 cells, and then observed EGFP expression 48 h after transfection.

EGFP signals were observed using a fluorescence microscope (EVOS FL, ThermoFisher, Waltham, MA, USA). Fluorescence intensity was quantified by Image J. NanoLuc luciferase activity was measured using the Nano-Light luciferase Reporter Assay kit (Meilunbio, Dalian, China). Firefly luciferase activity was measured using the Bright-Lite Luciferase Assay System (Vazyme, Nanjing, China).

2.5. RNA secondary structure analysis

Using RNAfold [RNAfold web server (univie.ac.at)] for RNA secondary structure prediction of minigenome sequences with only different terminal bases.

2.6. Remdesivir inhibition activity assay

Remdesivir (GS-5734) was purchased from Selleck (USA). The compound was dissolved in dimethyl sulfoxide (DMSO) according to the manufacturer's recommendations and stored until use. The MLAV minigenome containing the NanoLuc reporter and support plasmids was transfected into HEK293 cells as described above. Nine hours after transfection, the cell culture medium containing plasmids and transfection reagents was replaced with medium containing the remdesivir or DMSO, and the cells were incubated in cell incubator with 5% CO_2 at 37 °C for 24 h. Then, the cell culture medium was removed, the cells were washed with phosphate-buffered saline, and luciferase activity was measured. The inhibition% was calculated using the following equation: inhibition rate (%) = (Experimental group fluorescence value – average fluorescence value of drug control well)/(average fluorescence value of cell control well – average fluorescence value of drug control well) × 100.

2.7. Statistical analysis

Values in the texts and figures are presented as the mean ± standard error of mean (SEM). To compare whether the MLAV minigenome system depends on VP30, we performed a one-way repeated measures analysis of variance (ANOVA) followed by a paired *t*-test to compare the expression efficiency of the MLAV minigenome system with and without VP30. Data were analyzed by GraphPad Prism v8.0 (GraphPad Software Inc. San Diego, CA, USA). *P* values < 0.05 were considered statistically significant. *, $P < 0.05$; **, $P < 0.01$; ***, $P < 0.001$; ****, $P < 0.0001$.

3. Results

3.1. Complete genome of MLAV at the 3′-leader and 5′-trailer sequences

The published MLAV sequence (GenBank: NC_055510.1) lacks the leader and trailer sequences, which are critical for viral RNA synthesis (Fig. 1A). Using the RACE technology, we obtained the MLAV 3′-leader and 5′-trailer sequences, with lengths of 48 and 207 bp (GenBank: KX371887.3), respectively (Fig. 1A). MLAV shares a conserved gene start signal sequence and the 5′-end of the trailer sequence with other filoviruses (Fig. 1B and C). We found two variations (CC, CU) at the end of the 5′-trailer sequence; the CU sequence is unique to MLAV, and CC is present in the RESTV and MARV genomes, different from the CCU sequence in Bombali virus and the CCA sequence in the other filoviruses.

3.2. Generation of an authentic MLAV minigenome

In our previous study, we developed chimeric MLAV minigenomes that carried the 3′-leader and 5′-trailer sequences of EBOV and MARV (Yang et al., 2019). Here, we used a similar strategy to construct a MLAV minigenome using the newly obtained 3′-leader and 5′-trailer sequences of MLAV, carrying the CC nucleotides at the end of the 5′-trailer (Fig. 2A).

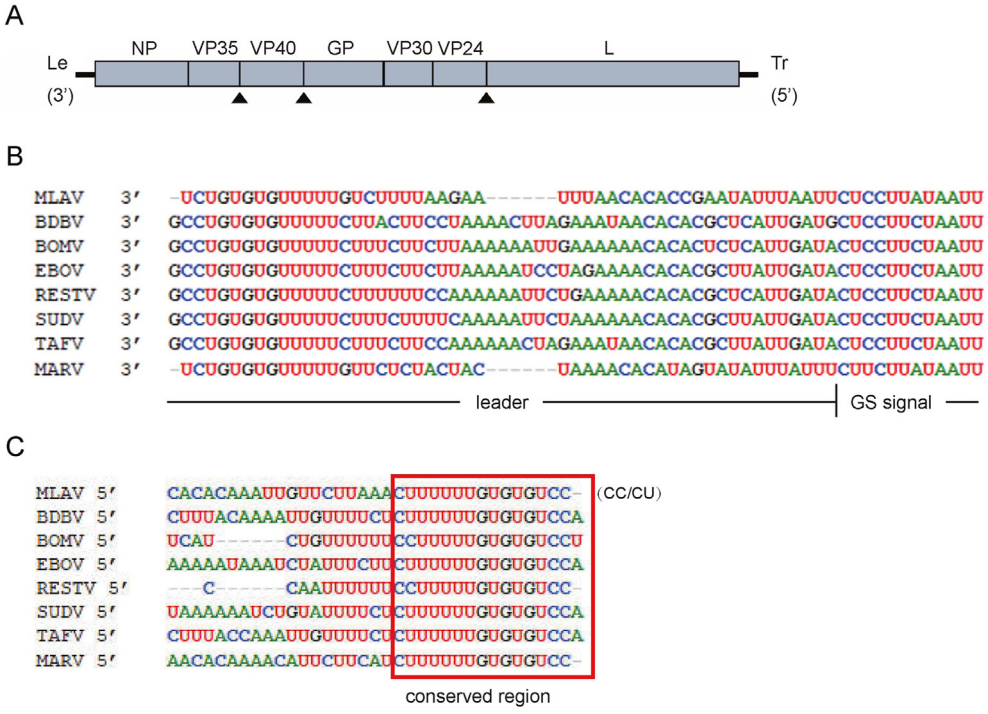

Fig. 1. Genome comparison of Měnglà virus (MLAV) and other mammal filoviruses. **A** Schematic representation of the MLAV genome. Solid black lines indicate the leader (Le) and trailer (Tr). Open reading frames are shown as gray boxes. Black triangles indicate sites of gene overlap. **B** Comparison of 3′ genome ends of filovirus species. Sequences of the leaders and *NP* gene start (GS) signals are shown. **C** Comparison of 5′ genome ends of filovirus species. Trailer sequences are shown. BDBV, Bundibugyo virus; BOMV, Bombali virus; EBOV, Ebola virus; RESTV, Reston virus; SUDV, Sudan virus; TAFV, Tai Forest virus; MARV, Marburg virus. The polymorphic nucleotide sites at the end of the MLAV genome are shown in parentheses.

We optimized all components, including the support plasmids (NP, VP35, VP30, L, and T7) and MLAV minigenome, and got the best plasmid ratio for the luminescence activity of MLAV minigenome replication system: 350 ng NP, 100 ng VP35, 30 ng VP30, 260 ng L, 500 ng minigenome plasmid (MG), and 125 ng T7 polymerase plasmid (Fig. 2B and C).

3.3. MLAV minigenome transcription is independent of VP30

Although both EBOV and MARV belong to the *Filoviridae* family and share many similarities in their replication and transcription strategies, there are also significant differences. VP30 is necessary for EBOV and RESTV minigenome transcription (Muhlberger et al., 1999; Boehmann et al., 2005), but not for that of MARV (Muhlberger et al., 1998; Albarino et al., 2013). However, VP30 is required for rescuing full-length infectious cDNA clones of MARV and EBOV (Volchkov et al., 2001; Enterlein et al., 2006). Studies have shown that EBOV and MARV can interchange VP30 to maintain transcriptional competence (Muhlberger et al., 1999; Boehmann et al., 2005; Enterlein et al., 2006). The chimeric Lloviu virus minigenome has a similar transcriptional strategy as EBOV, and its activity is significantly enhanced by the presence of VP30 protein (Manhart et al., 2018). In this study, we transfected cells with the MLAV minigenome and MLAV polymerase complex plasmids lacking VP30. In the

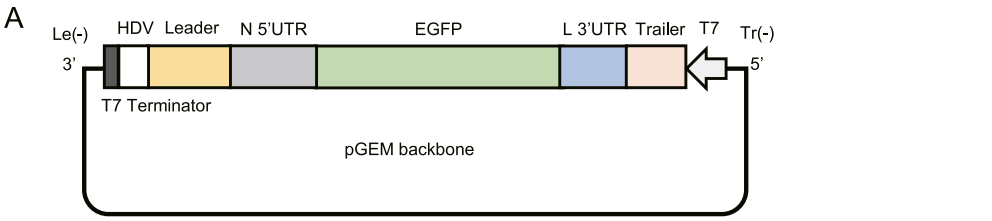

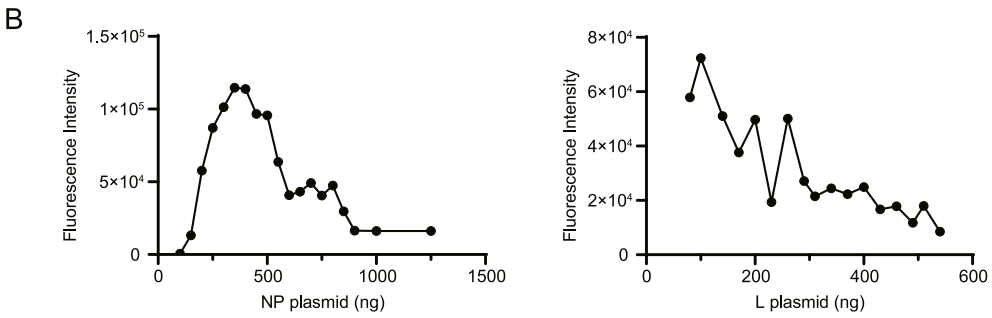

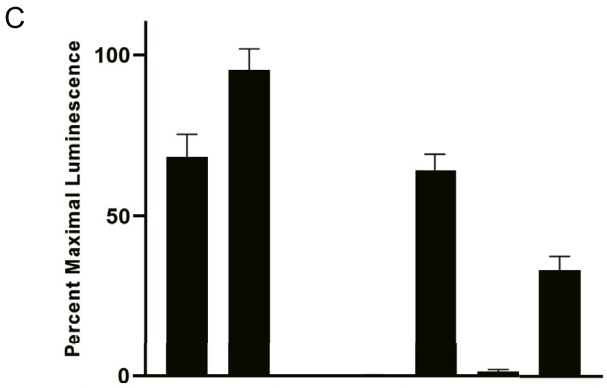

NP	300	350	350	350	350	350	350
VP35	50	100	500	1000	100	500	50
VP30	30	30	50	50	100	30	200
L	100	260	100	100	100	100	100
T7	125	125	125	125	125	125	125
MG	500	500	500	500	1000	1000	1000

Fig. 2. Generation and optimization of the MLAV minigenome system. **A** Map of the MLAV minigenome composed of the T7 termination signal, hepatitis delta virus (HDV) ribozyme, MLAV leader sequence, *NP* gene 5′ UTR region, EGFP reporter gene, *L* gene 3′ UTR region, MLAV trailer sequence, and T7 polymerase. The MLAV 3′-leader (3) and 5′-trailer (5) are the sequences of MLAV obtained in this study, carrying the CC nucleotides at the end of the 5′-trailer. **B** Optimization on the amounts of NP and L plasmids in the minigenome replication system. HEK293 cells were co-transfected with NP and L plasmid (ranged from 50 ng to 1.5 μg), minigenome plasmid (500 ng), VP35 (62.5 ng), VP30 (37.5 ng), and pCAGGS-T7/Pol plasmid expressing the T7 RNA polymerase (125 ng). Fluorescence intensity was determined at 48 h post-transfection by Image J. All assays were repeated twice. **C** Combinations with different amounts of support plasmids and the minigenome (MG) plasmid were assessed. The minigenome activity for each combination is represented as a percentage of maximal luminescence. The amount of each plasmid (ng) is shown below the bar graph. The assays were repeated in triplicate. Data presented as means ± SEM.

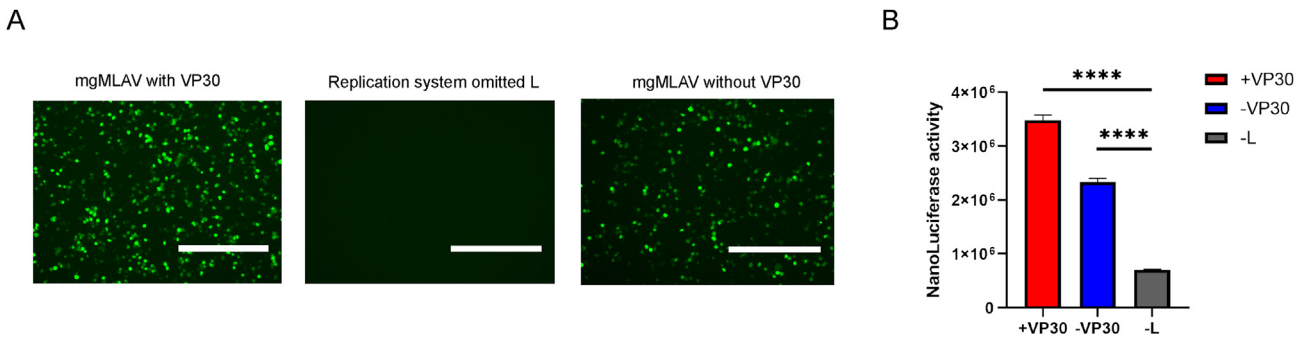

Fig. 3. MLAV minigenome transcription activity is independent of VP30. **A** HEK293 cells were co-transfected with MLAV EGFP minigenome (mgMLAV) plasmid and support plasmids with or without VP30. The replication system omitted L plasmid was set as the negative control. The experiment was repeated three times. Representative fluorescence images at 48 h post-transfection are shown (scale bars, 400 μm). **B** The activity of MLAV minigenome system with Nanoluc reporter gene. Data presented as means ± SEM. One-way repeated measures analysis of variance (ANOVA) followed by a paired *t*-test were performed (****$P < 0.0001$).

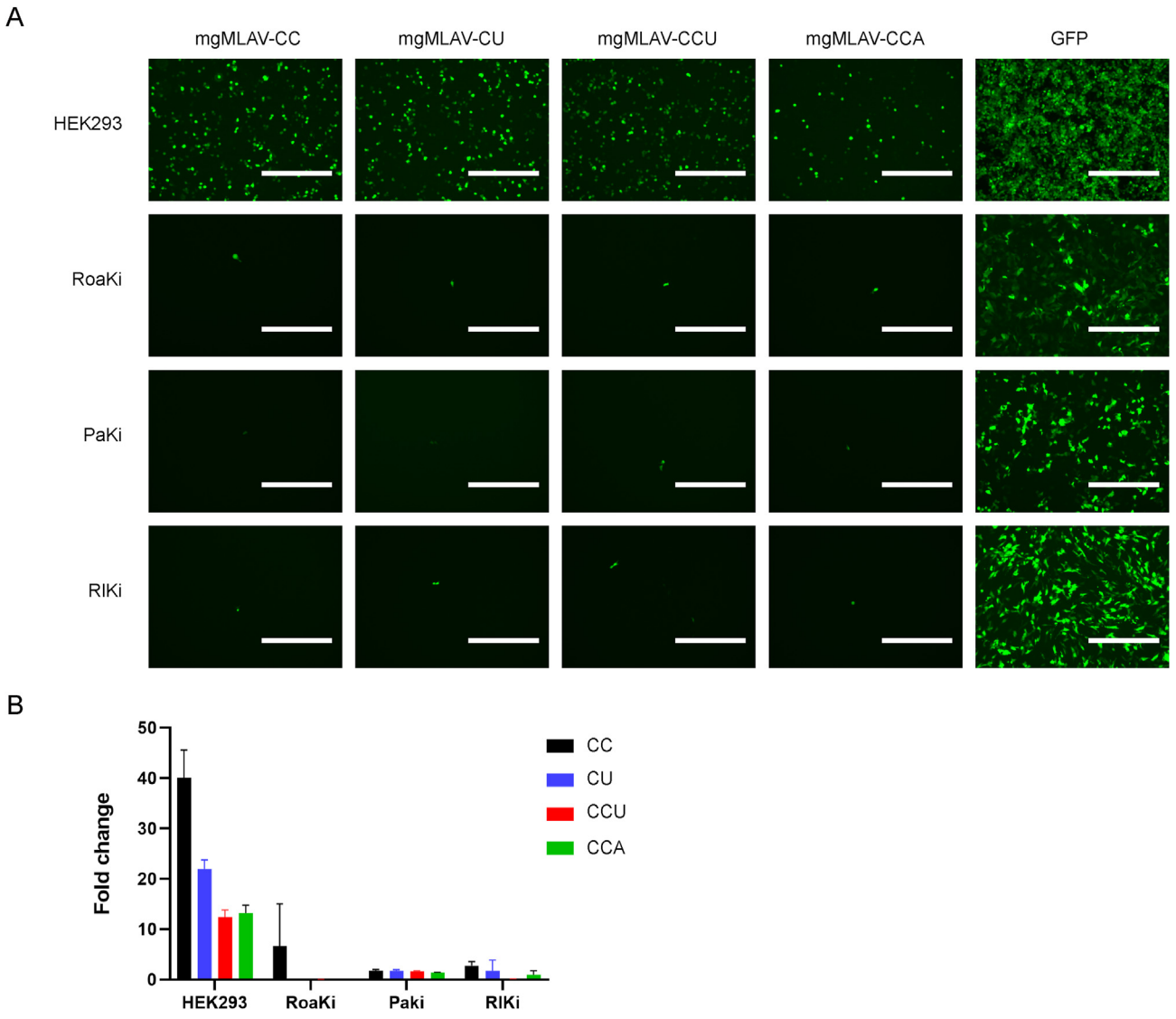

Fig. 4. The end bases of MLAV genome affect RNA synthesis efficiency of minigenome. **A** EGFP-expressing MLAV minigenomes (mgMLAV) containing different terminal sequences were transfected into HEK293 cells or bats' cells [*Rousettus amplexicaudatus* (RoaKi), *Rousettus leschenaultia* (RlKi), and *Pteropus alecto* (PaKi)] along with the MLAV replication complexes. Representative fluorescence images at 48 h post-transfection are shown (scale bars, 400 μm). **B** Nanoluc-expressing MLAV minigenomes containing different terminal sequences and MLAV replication complexes into HEK293 cells or bat cells [*Rousettus amplexicaudatus* (RoaKi), *Rousettus leschenaultia* (RlKi) and *Ptropus alecto* (PaKi)]. The pNL4-3-luc-R-E plasmid expressing firefly luciferase was co-transfected as the internal control for transfection efficiency. Cells were harvested at 48 h post-transfection to determine the luciferase activity. The fold change was calculated using the following equation: Nanoluc fluorescence value in experimental group/fluorescence value of firefly luciferase. Data presented as the means ± SEM from three independent experiments.

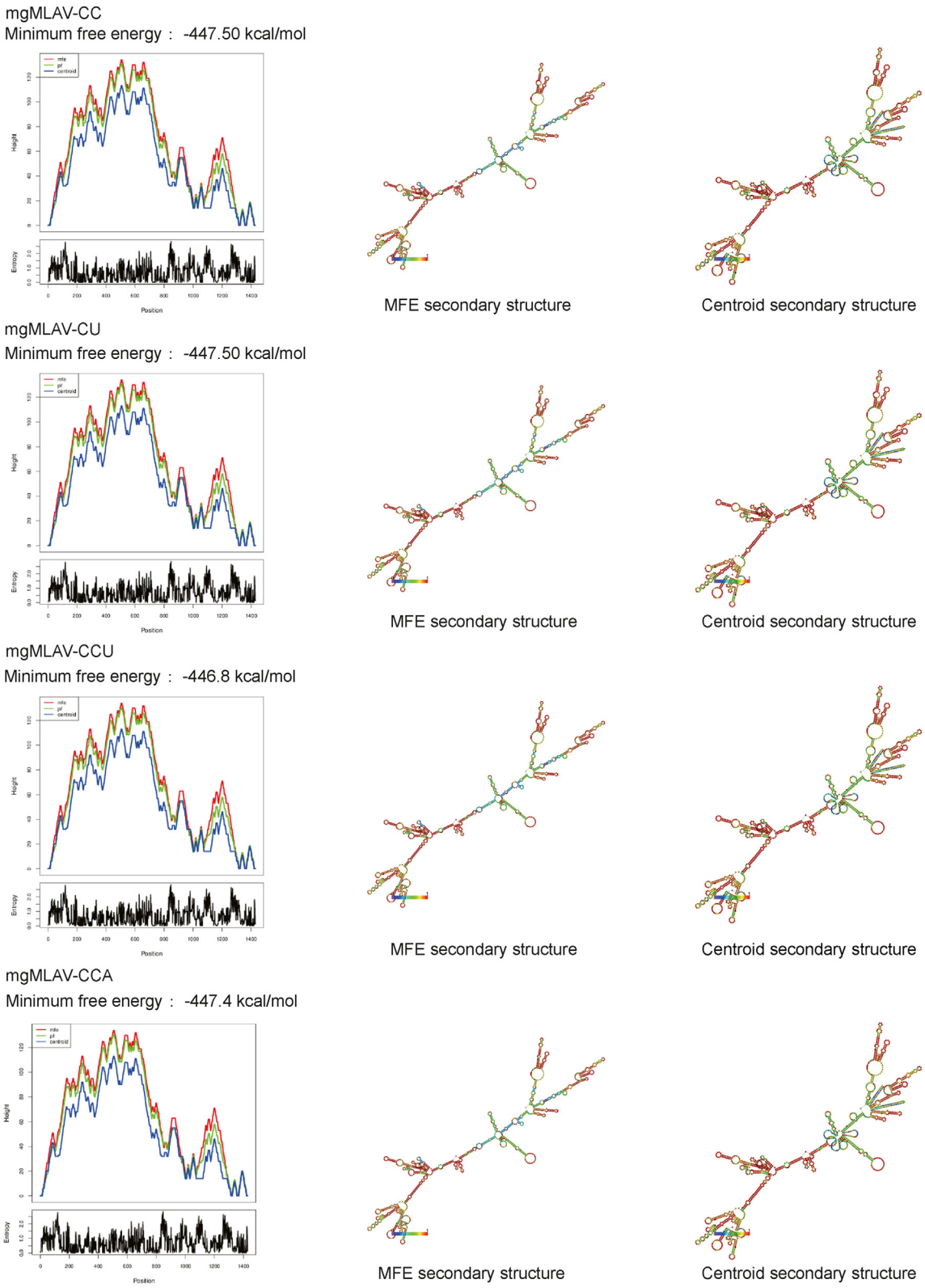

Fig. 5. RNA secondary structures of minigenomes containing different terminal bases. Schematic diagram showing the secondary structure of terminal base RNA. The RNA secondary structure was predicted using the RNAfold software.

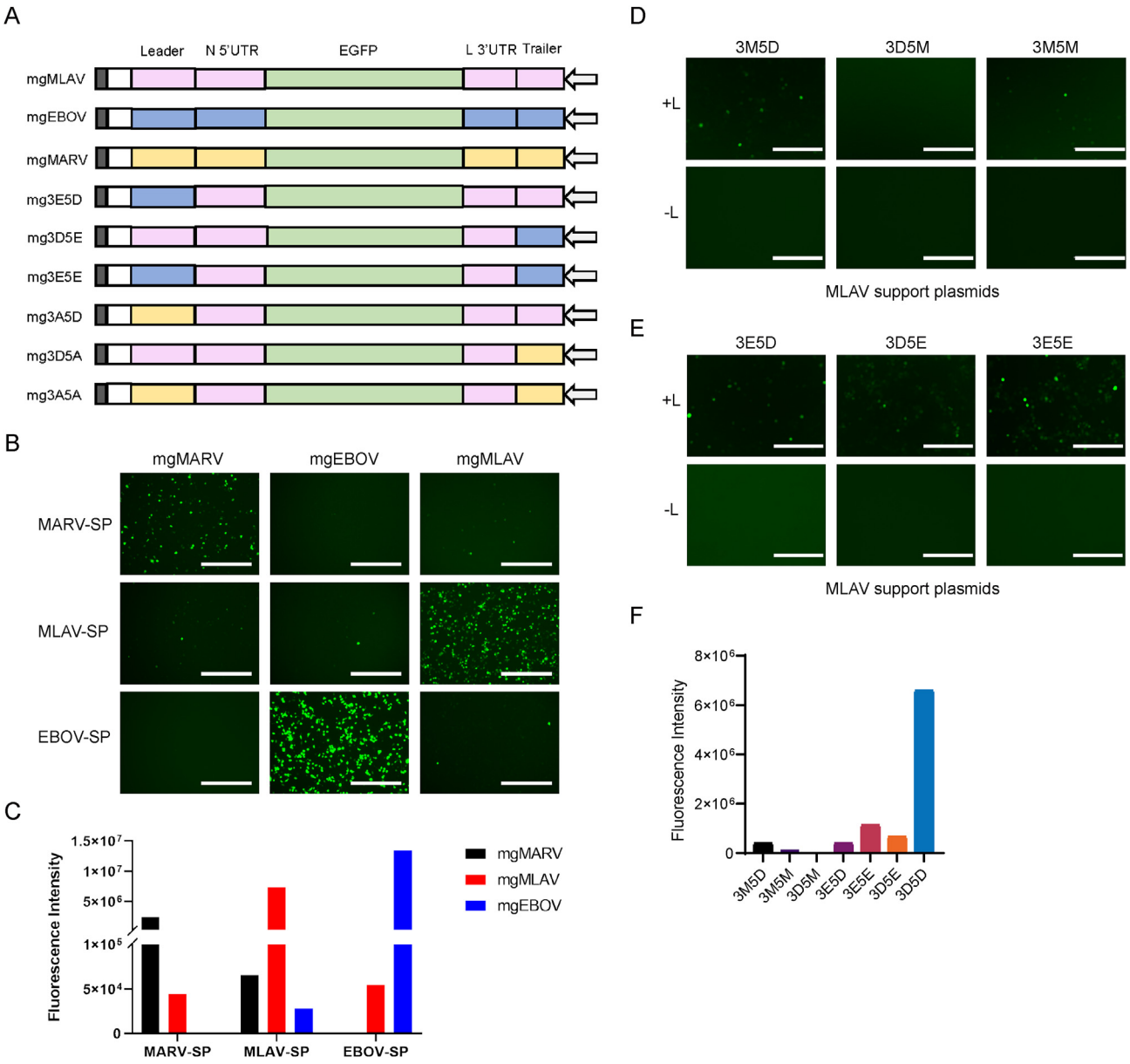

Fig. 6. MLAV replication complexes can recognize other filovirus minigenomes. **A** Schemes of the chimeric minigenomes. The EGFP reporter gene was flanked by the 3′-leader of EBOV or MARV, the non-coding region (NCR) of the MLAV *NP* gene (N 5′ UTR), the NCR of the MLAV *L* gene (L 3′ UTR), and 5′-trailer of EBOV or MARV. 3E5D: 3′-leader of EBOV and 5′-trailer of MLAV; 3D5E: 3′-leader of MLAV and 5′-trailer of EBOV; 3E5E: 3′-leader of EBOV and 5′-trailer of EBOV; 3M5D: 3′-leader of MARV and 5′-trailer of MLAV; 3D5M: 3′-leader of MLAV and 5′-trailer of MARV; 3M5M: 3′-leader of MARV and 5′-trailer of MLAV. Pink: MLAV minigenome, Blue: EBOV minigenome, Yellow: MARV minigenome. **B, C** HEK293 cells were transfected with polymerase complex from MARV, EBOV, and MLAV combined with homologous and heterologous support plasmids (SP). Each polymerase complex was used at its own optimal concentration. Representative fluorescence images at 48 h post-transfection are shown (scale bars, 400 μm). Images were analyzed using ImageJ and the fluorescence intensities were quantified. **D, E** HEK293 cells were transfected with MLAV polymerase complex and different EGFP-expressing chimeric minigenomes with MARV or EBOV leader and trailer sequences. Representative fluorescence images at 48 h post-transfection are shown (scale bars, 200 μm). **F** Quantitative fluorescence results of the images in **D** and **E**. The images were analyzed using ImageJ.

absence of VP30, MLAV minigenome can also process transcription course (Fig. 3).

3.4. RNA synthesis activity of the MLAV minigenome is higher in human cells than in bat cells

MLAV was discovered in *Rousettus amplexicaudatus*, which cohabit caves with other bat species, such as *Rousettus leschenaultia*. We investigated whether the RNA synthesis efficiency of MLAV minigenome varies among cells of different species. The MLAV minigenome was transfected into HEK293 cells and immortalized renal cells from *R. amplexicaudatus* (RoaKi), *R. leschenaultia* (RlKi), and *Pteropus alecto* (PaKi). Minigenome reporter activity was assessed by measuring reporter gene expression at 48 h post-transfection. The results showed that MLAV minigenome reporter activity was significantly lower in bat's cells than in human-derived cells (Fig. 4A and B).

3.5. Nucleotide variation in the 5′-trailer sequence affects RNA synthesis activity of MLAV minigenome

We detected two nucleotide polymorphisms (CC and CU) near the end of the MLAV 5′-trailer sequence. To investigate whether these differences in

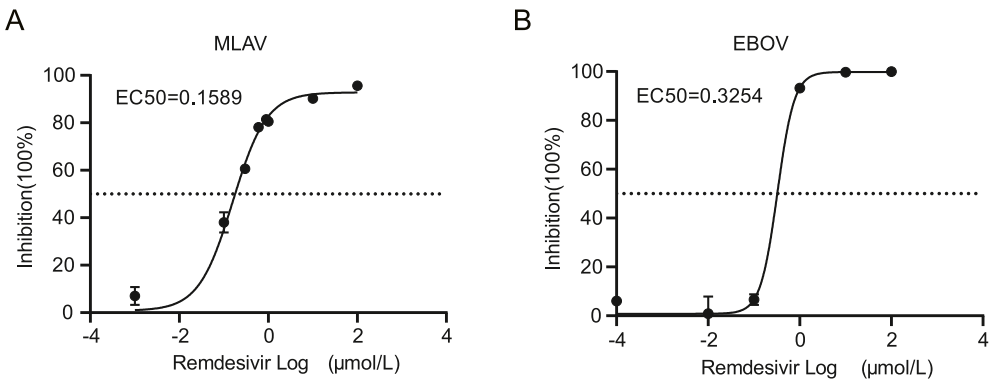

Fig. 7. Remdesivir inhibition assay in minigenome systems. The MLAV and EBOV minigenome containing the NanoLuc reporter and related support plasmids were transfected into HEK293 cells. The cell culture medium was replaced with the medium containing remdesivir or DMSO at 9 h post-transfection. Cells were harvested and lysed at 24 h post-transfection. The NanoLuc luciferase activity was measured. The inhibition% was calculated using the following equation: inhibition rate (%) = (Experimental group fluorescence value − average fluorescence value of drug control well)/(average fluorescence value of cell control well − average fluorescence value of drug control well) × 100. Data presented as the means ± SEM from three independent experiments.

the terminal sequence would affect the RNA synthesis activity of the MLAV minigenome, we constructed MLAV minigenomes containing these two sequences, and set the CCA and CCU sequences as controls. The EGFP expression levels of MLAV variant minigenomes were assessed in HEK293 cells and different bat's cells. No differences were observed in EGFP expression, except for the MLAV minigenomes containing CCA or CCU ends, which produced slightly lower fluorescence intensity than the other sequences (Fig. 4A and B).

Secondary structural modeling showed that the free energy values of the sequences containing the CC or CU ends were lower than those of the sequences containing CCU or CCA at the end, suggesting that the RNA secondary structures containing CC and CU termini are more stable (Fig. 5).

3.6. EBOV and MRAV 3′-leader sequences are compatible with the MLAV polymerase complex

Polymerase complexes of related viruses can recognize each other (Theriault et al., 2004; Boehmann et al., 2005). We assessed the compatibility of the replication complex and minigenome among the three filoviruses (Fig. 6A–C). The filovirus minigenomes were highly compatible with their own replication complex. The MLAV replication complex supported not only its own minigenome, but also those of MARV and EBOV, albeit less efficiently. Similarly, the MLAV minigenome recognized the replication complexes of MARV and EBOV, albeit with weak replication or transcription.

To investigate the compatibility of the MLAV replication complex with the leader and trailer sequences of EBOV and MARV, chimeric minigenomes were designed, replacing the 3′-leader and 5′-trailer sequences of MLAV with those of EBOV and MARV (Fig. 6D–F). The results showed that the MLAV replication complex was able to transcribe chimeric minigenomes with leader and trailer sequences of MARV and EBOV, albeit with low efficiency.

3.7. Antiviral drug testing using the MLAV minigenome

The minigenome system provides a convenient and rapid platform for high-throughput *in vitro* drug screening of highly pathogenic viruses, without the requirement for live virus manipulation in a high-level biosafety laboratory (Brown et al., 2014; Edwards et al., 2015; McCarthy et al., 2016; Nelson et al., 2017; Du et al., 2020). We tested the inhibitory activity of remdesivir (GS-5734), which targets the RNA-dependent RNA polymerase of EBOV and other RNA viruses (Lo et al., 2017; Siegel et al., 2017; Brown et al., 2019; Lo et al., 2020; Bodmer et al., 2021). We found that it also inhibits genome replication with no significant difference compared to EBOV (Fig. 7A and B).

4. Discussion

In this study, we sequenced the 5′- and 3′-ends to complete the MLAV genome sequence. MLAV shares conserved sequences in the cis-acting regulatory elements and conserved regions at the 5′-end of the genome with other filoviruses. We identified two variants in the 5′-end of the MLAV genome, which did not affect reporter activity. However, the MLAV minigenome showed slightly reduced reporter activity when these variants were replaced with the CCA or CCU sequences carried by most filoviruses. We hypothesized that the CCA and CCU terminal sequences are heterologous and therefore adversely affect minigenome RNA synthesis. We tested the reporter activity of these four termini in the MLAV minigenome in different cells, and found that RNA synthesis of the MLAV minigenome was more efficient in human cells than in bat cells. This phenomenon may be due to MLAV restricting transcription or replication in its natural host, but it is probably well adapted to human cells. It may also have resulted from our optimization on the plasmid ratio of the minigenome system in HEK293, which led to better reporter gene expression. Another potential explanation is that the protein expression efficiency of plasmids in bat cells may be lower than in human cells, due to the co-transfection of multiple plasmids.

It has been demonstrated that the leader and trailer sequences in filovirus genomes affect the RNA synthesis of the minigenome (Bach et al., 2021). We assessed the compatibility of different filovirus minigenomes with both homogenous and heterogeneous leader and trailer sequences. The reporter efficiency of the MLAV polymerase complex was the highest when the minigenome system contained its own 3′-leader and 5′-trailer sequences. Although the MLAV polymerase complex exhibited greater efficiency in transcribing the 3′-leader and 5′-trailer sequences of EBOV compared to those of MARV, substituting the 3′-leader and 5′-trailer sequences of MLAV with those of MARV or EBOV, or with recombinant leader and trailer sequences, led to the decreased reporter activity. These results are consistent with previous findings that the nucleotide sequences of filovirus 3′-leader are associated with the species specificity of filovirus polymerases (Manhart et al., 2018).

Functional analysis on the polymerase protein of MLAV revealed that its innate immune evasion mechanism is similar to that of MARV and more closely related to MARV than to EBOV (Williams et al., 2020). VP30 is an important transcription factor for filovirus genome synthesis. While the transcription of EBOV and RESTV heavily relies on VP30 (Muhlberger et al., 1999; Boehmann et al., 2005), this is not the case for the MARV minigenome system (Muhlberger et al., 1998; Albarino et al., 2013). Our study

demonstrated that MLAV minigenome transcription is independent of VP30, suggesting that MLAV and MARV share some common biological features. The compatibility of transcription or replication mechanisms is also demonstrated by the mutual recognition between filovirus minigenomes and polymerase complexes of other species (Theriault et al., 2004; Boehmann et al., 2005). Our study also demonstrated that the polymerase complexes and minigenomes of MLAV, EBOV, and MARV have low compatibility in heterogeneous recombination. Nevertheless, MLAV polymerase complex supported RNA synthesis of EBOV and MARV minigenomes with low efficiency, which was not observed between EBOV and MARV.

5. Conclusions

In this study, we utilized the optimized MLAV minigenome system to assess the *in vitro* efficacy of remdesivir. It reportedly inhibits the RNA synthesis activity of EBOV minigenome or virus and other RNA viruses, such as SARS-related coronaviruses (Malin et al., 2020). Our results showed that remdesivir has a similar inhibitory effect on MLAV and EBOV. This study demonstrates the usefulness of the MLAV minigenome system for future studies of MLAV transcription and replication mechanisms, as well as for antiviral drug screening.

Data availability

All the data generated during the current study are included in the manuscript. The full-length sequence of Měnglà virus in this study is available in the Science Data Bank: https://doi.org/10.57760/sciencedb.18451.

Ethics statement

This article does not contain any studies with human or animal subjects performed by any of the authors.

Author contributions

Shi-Zhe Xie: conceptualization, data curation, investigation, methodology, software, writing-original draft. Ke Yao: investigation. Bei Li: investigation. Cheng Peng: investigation. Xing-Lou Yang: conceptualization, data curation, methodology, validation, writing-review & editing. Zheng-Li Shi: conceptualization, funding acquisition, supervision, writing-review & editing.

Conflict of interest

Prof. Zheng-Li Shi is the Editor-in-Chief for *Virologica Sinica* and was not involved in the editorial review or the decision to publish this article. The authors declare that they have no conflict of interest.

Acknowledgements

This work was jointly supported by the Key project of the Chinese Academy of Sciences (KJZD-SW-L11 to Z.-L.S.), the Guangzhou Laboratory (SRPG22-001 to Z.-L.S.), the Advanced Customer Cultivation Project of Wuhan National Biosafety Laboratory, Chinese Academy of Sciences (2021ACCP-MS02), the Strategic Priority Research Program of the Chinese Academy of Sciences (XDB0490000 to X.-L.Y.), the Young Top-notch Talent Cultivation Program of Hubei Province (X.-L.Y.), the Youth Innovation Promotion Association of the Chinese Academy of Science (X.-L.Y.).

References

Albarino, C.G., Uebelhoer, L.S., Vincent, J.P., Khristova, M.L., Chakrabarti, A.K., McElroy, A., Nichol, S.T., Towner, J.S., 2013. Development of a reverse genetics system to generate recombinant marburg virus derived from a bat isolate. Virology 446, 230–237.

Bach, S., Demper, J.C., Klemm, P., Schlereth, J., Lechner, M., Schoen, A., Kaemper, L., Weber, F., Becker, S., Biedenkopf, N., Hartmann, R.K., 2021. Identification and characterization of short leader and trailer RNAs synthesized by the Ebola virus RNA polymerase. PLoS Pathog. 17, e1010002.

Bodmer, B.S., Zierke, L., Wendt, L., Gressler, J., Groseth, A., Hoenen, T., 2021. Remdesivir inhibits the polymerases of the novel filoviruses Lloviu and Bombali virus. Antiviral Res. 192, 105120.

Boehmann, Y., Enterlein, S., Randolf, A., Muhlberger, E., 2005. A reconstituted replication and transcription system for Ebola virus reston and comparison with Ebola virus zaire. Virology 332, 406–417.

Brown, A.J., Won, J.J., Graham, R.L., Dinnon, K.H., Sims, A.C., Feng, J.Y., Cihlar, T., Denison, M.R., Baric, R.S., Sheahan, T.P., 2019. Broad spectrum antiviral remdesivir inhibits human endemic and zoonotic deltacoronaviruses with a highly divergent RNA dependent rna polymerase. Antiviral Res. 169, 104541.

Brown, C.S., Lee, M.S., Leung, D.W., Wang, T., Xu, W., Luthra, P., Anantpadma, M., Shabman, R.S., Melito, L.M., MacMillan, K.S., Borek, D.M., Otwinowski, Z., Ramanan, P., Stubbs, A.J., Peterson, D.S., Binning, J.M., Tonelli, M., Olson, M.A., Davey, R.A., Ready, J.M., Basler, C.F., Amarasinghe, G.K., 2014. In silico derived small molecules bind the filovirus VP35 protein and inhibit its polymerase cofactor activity. J. Mol. Biol. 426, 2045–2058.

Cao, Z., Liu, C., Peng, C., Ran, Y., Yao, Y., Xiao, G., Li, E., Chen, Z., Chuai, X., Chiu, S., 2023. Ebola virus VP35 perturbs type I interferon signaling to facilitate viral replication. Virol. Sin. 38, 922–930.

Crameri, G., Todd, S., Grimley, S., McEachern, J.A., Marsh, G.A., Smith, C., Tachedjian, M., De Jong, C., Virtue, E.R., Yu, M., Bulach, D., Liu, J.P., Michalski, W.P., Middleton, D., Field, H.E., Wang, L.F., 2009. Establishment, immortalisation and characterisation of pteropid bat cell lines. PLoS One 4, e8266.

Deflube, L.R., Cressey, T.N., Hume, A.J., Olejnik, J., Haddock, E., Feldmann, F., Ebihara, H., Fearns, R., Muhlberger, E., 2019. Ebolavirus polymerase uses an unconventional genome replication mechanism. Proc. Natl. Acad. Sci. U. S. A. 116, 8535–8543.

Du, X.H., Zuo, X.Y., Meng, F., Wu, F., Zhao, X., Li, C.F., Cheng, G.H., Qin, F.X.F., 2020. Combinatorial screening of a panel of FDA-approved drugs identifies several candidates with anti-Ebola activities. Biochem. Biophys. Res. Commun. 522, 862–868.

Edwards, M.R., Pietzsch, C., Vausselin, T., Shaw, M.L., Bukreyev, A., Basler, C.F., 2015. High-throughput minigenome system for identifying small-molecule inhibitors of Ebola virus replication. ACS Infect. Dis. 1, 380–387.

Enterlein, S., Volchkov, V., Weik, M., Kolesnikova, L., Volchkova, V., Klenk, H.D., Muhlberger, E., 2006. Rescue of recombinant Marburg virus from cDNA is dependent on nucleocapsid protein VP30. J. Virol. 80, 1038–1043.

Hoenen, T., Groseth, A., de Kok-Mercado, F., Kuhn, J.H., Wahl-Jensen, V., 2011. Minigenomes, transcription and replication competent virus-like particles and beyond: reverse genetics systems for filoviruses and other negative stranded hemorrhagic fever viruses. Antiviral Res. 91, 195–208.

Horie, M., 2021. Identification of a novel filovirus in a common lancehead (bothrops atrox (linnaeus, 1758)). J. Vet. Med. Sci. 83, 1485–1488.

Kemenesi, G., Toth, G.E., Mayora-Neto, M., Scott, S., Temperton, N., Wright, E., Muhlberger, E., Hume, A.J., Suder, E.L., Zana, B., Boldogh, S.A., Gorfol, T., Estok, P., Lanszki, Z., Somogyi, B.A., Nagy, A., Pereszlenyi, C.I., Dudas, G., Foldes, F., Kurucz, K., Madai, M., Zeghbib, S., Maes, P., Vanmechelen, B., Jakab, F., 2022. Isolation of infectious Lloviu virus from Schreiber's bats in Hungary. Nat. Commun. 13, 1706.

Koch, L.K., Cunze, S., Kochmann, J., Klimpel, S., 2020. Bats as putative Zaire ebolavirus reservoir hosts and their habitat suitability in Africa. Sci. Rep. 10, 14268.

Kuhn, J.H., Amarasinghe, G.K., Basler, C.F., Bavari, S., Bukreyev, A., Chandran, K., Crozier, I., Dolnik, O., Dye, J.M., Formenty, P.B.H., Griffiths, A., Hewson, R., Kobinger, G.P., Leroy, E.M., Muhlberger, E., Netesov Нетёсов Сергей Викторович, S.V., Palacios, G., Palyi, B., Paweska, J.T., Smither, S.J., Takada, A., Towner, J.S., Wahl, V., ICTV Report Consortium, 2019. Ictv virus taxonomy profile: Filoviridae. J. Gen. Virol. 100, 911–912.

Lo, M.K., Jordan, R., Arvey, A., Sudhamsu, J., Shrivastava-Ranjan, P., Hotard, A.L., Flint, M., McMullan, L.K., Siegel, D., Clarke, M.O., Mackman, R.L., Hui, H.C., Perron, M., Ray, A.S., Cihlar, T., Nichol, S.T., Spiropoulou, C.F., 2017. GS-5734 and its parent nucleoside analog inhibit filo-, pneumo-, and paramyxoviruses. Sci. Rep. 7, 43395.

Lo, M.K., Albarino, C.G., Perry, J.K., Chang, S., Tchesnokov, E.P., Guerrero, L., Chakrabarti, A., Shrivastava-Ranjan, P., Chatterjee, P., McMullan, L.K., Martin, R., Jordan, R., Gotte, M., Montgomery, J.M., Nichol, S.T., Flint, M., Porter, D., Spiropoulou, C.F., 2020. Remdesivir targets a structurally analogous region of the Ebola virus and SARS-Cov-2 polymerases. Proc. Natl. Acad. Sci. U. S. A. 117, 26946–26954.

Luo, Y., Chen, Y., Geng, R., Li, B., Chen, J., Zhao, K., Zheng, X.S., Zhang, W., Zhou, P., Yang, X.L., Shi, Z.L., 2021. Broad cell tropism of SADS-Cov *in vitro* implies its potential cross-species infection risk. Virol. Sin. 36, 559–563.

Malin, J.J., Suarez, I., Priesner, V., Fatkenheuer, G., Rybniker, J., 2020. Remdesivir against COVID-19 and other viral diseases. Clin. Microbiol. Rev. 34, e00162-20.

Manhart, W.A., Pacheco, J.R., Hume, A.J., Cressey, T.N., Deflube, L.R., Muhlberger, E., 2018. A chimeric Lloviu virus minigenome system reveals that the bat-derived filovirus replicates more similarly to ebolaviruses than marburgviruses. Cell Rep. 24, 2573–2580.e4.

Martin, B., Canard, B., Decroly, E., 2017. Filovirus proteins for antiviral drug discovery: structure/function bases of the replication cycle. Antiviral Res. 141, 48–61.

McCarthy, S.D., Majchrzak-Kita, B., Racine, T., Kozlowski, H.N., Baker, D.P., Hoenen, T., Kobinger, G.P., Fish, E.N., Branch, D.R., 2016. A rapid screening assay identifies

monotherapy with interferon-ß and combination therapies with nucleoside analogs as effective inhibitors of Ebola virus. PLoS Negl. Trop. Dis. 10, e0004364.
Muhlberger, E., 2007. Filovirus replication and transcription. Future Virol. 2, 205–215.
Muhlberger, E., Lotfering, B., Klenk, H.D., Becker, S., 1998. Three of the four nucleocapsid proteins of Marburg virus, NP, VP35, and L, are sufficient to mediate replication and transcription of Marburg virus-specific monocistronic minigenomes. J. Virol. 72, 8756–8764.
Muhlberger, E., Weik, M., Volchkov, V.E., Klenk, H.D., Becker, S., 1999. Comparison of the transcription and replication strategies of Marburg virus and Ebola virus by using artificial replication systems. J. Virol. 73, 2333–2342.
Negredo, A., Palacios, G., Vazquez-Moron, S., Gonzalez, F., Dopazo, H., Molero, F., Juste, J., Quetglas, J., Savji, N., de la Cruz Martinez, M., Herrera, J.E., Pizarro, M., Hutchison, S.K., Echevarria, J.E., Lipkin, W.I., Tenorio, A., 2011. Discovery of an ebolavirus-like filovirus in europe. PLoS Pathog. 7, e1002304.
Nelson, E.V., Pacheco, J.R., Hume, A.J., Cressey, T.N., Deflube, L.R., Ruedas, J.B., Connor, J.H., Ebihara, H., Muhlberger, E., 2017. An RNA polymerase II-driven Ebola virus minigenome system as an advanced tool for antiviral drug screening. Antiviral Res. 146, 21–27.
Olival, K.J., Hayman, D.T., 2014. Filoviruses in bats: current knowledge and future directions. Viruses 6, 1759–1788.
Rougeron, V., Feldmann, H., Grard, G., Becker, S., Leroy, E.M., 2015. Ebola and marburg haemorrhagic fever. J. Clin. Virol. 64, 111–119.
Shi, M., Lin, X.D., Chen, X., Tian, J.H., Chen, L.J., Li, K., Wang, W., Eden, J.S., Shen, J.J., Liu, L., Holmes, E.C., Zhang, Y.Z., 2018. The evolutionary history of vertebrate RNA viruses. Nature 556, 197–202.
Siegel, D., Hui, H.C., Doerffler, E., Clarke, M.O., Chun, K., Zhang, L., Neville, S., Carra, E., Lew, W., Ross, B., Wang, Q., Wolfe, L., Jordan, R., Soloveva, V., Knox, J., Perry, J., Perron, M., Stray, K.M., Barauskas, O., Feng, J.Y., Xu, Y., Lee, G., Rheingold, A.L., Ray, A.S., Bannister, R., Strickley, R., Swaminathan, S., Lee, W.A., Bavari, S., Cihlar, T., Lo, M.K., Warren, T.K., Mackman, R.L., 2017. Discovery and synthesis of a phosphoramidate prodrug of a pyrrolo[2,1-f][triazin-4-amino] adenine C-nucleoside (GS-5734) for the treatment of Ebola and emerging viruses. J. Med. Chem. 60, 1648–1661.
Sztuba-Solinska, J., Diaz, L., Kumar, M.R., Kolb, G., Wiley, M.R., Jozwick, L., Kuhn, J.H., Palacios, G., Radoshitzky, S.R., Le Grice, S.F.J., Johnson, R.F., 2016. A small stem-loop structure of the Ebola virus trailer is essential for replication and interacts with heat-shock protein A8. Nucleic Acids Res. 44, 9831–9846.
Theriault, S., Groseth, A., Neumann, G., Kawaoka, Y., Feldmann, H., 2004. Rescue of Ebola virus from cDNA using heterologous support proteins. Virus Res. 106, 43–50.
Volchkov, V.E., Volchkova, V.A., Muhlberger, E., Kolesnikova, L.V., Weik, M., Dolnik, O., Klenk, H.D., 2001. Recovery of infectious Ebola virus from complementary DNA: RNA editing of the GP gene and viral cytotoxicity. Science 291, 1965–1969.
Watt, A., Moukambi, F., Banadyga, L., Groseth, A., Callison, J., Herwig, A., Ebihara, H., Feldmann, H., Hoenen, T., 2014. A novel life cycle modeling system for Ebola virus shows a genome length-dependent role of VP24 in virus infectivity. J. Virol. 88, 10511–10524.
Williams, C.G., Gibbons, J.S., Keiffer, T.R., Luthra, P., Edwards, M.R., Basler, C.F., 2020. Impact of Mĕnglà virus proteins on human and bat innate immune pathways. J. Virol. 94, e00191-20.
Yang, X.L., Tan, C.W., Anderson, D.E., Jiang, R.D., Li, B., Zhang, W., Zhu, Y., Lim, X.F., Zhou, P., Liu, X.L., Guan, W., Zhang, L., Li, S.Y., Zhang, Y.Z., Wang, L.F., Shi, Z.L., 2019. Characterization of a filovirus (Mĕnglà virus) from rousettus bats in China. Nat. Microbiol. 4, 390–395.